Fish and Shellfish Immunology 94 (2019) 455–463

Contents lists available at ScienceDirect

Fish and Shellfish Immunology

journal homepage: www.elsevier.com/locate/fsi

Full length article

Molecular characterization, tissue distribution and functional analysis of galectin 1-like 2 in grass carp (*Ctenopharyngodon idella*)

Denghui Zhu[a,b,1], Peipei Fu[b,d,1], Rong Huang[a], Lv Xiong[a,b], Yumeng Wang[e], Libo He[a], Lanjie Liao[a], Yongming Li[a], Zuoyan Zhu[a], Yaping Wang[a,c,*]

[a] State Key Laboratory of Freshwater Ecology and Biotechnology, Institute of Hydrobiology, Chinese Academy of Sciences, Wuhan, 430072, PR China
[b] University of Chinese Academy of Sciences, Beijing, 100049, PR China
[c] Innovative Academy of Seed Design, Chinese Academy of Sciences, Beijing, 100101, PR China
[d] Key Laboratory of Aquaculture Disease Control, Ministry of Agriculture, and State Key Laboratory of Freshwater Ecology and Biotechnology, Institute of Hydrobiology, Chinese Academy of Sciences, Wuhan, 430072, PR China
[e] Wuhan University, Wuhan, 430072, PR China

ARTICLE INFO

Keywords:
Galectin-1
Innate immunity
Grass carp reovirus
Microbial ligand binding
Subcellular localization

ABSTRACT

Galectins, as an evolutionary conserved group of lectin superfamily, has the functions of pathogen recognition, anti-bacteria and anti-virus. In this study, a 405 bp cDNA sequence of galectin 1-like 2 (*CiGal1-L2*) was obtained from grass carp (*Ctenopharyngodon idella*), which encoded 134 amino acids with a predicted molecular mass of 15.143 kDa and an isoelectric point of 5.33. The sugar binding motifs (H–N-R, V–N and W–E-R) were detected in carbohydrate-binding domain (CRD). The amino acid sequence similarity showed that CiGal1-L2 was 40.30–42.54% and 66.42–81.20% similarity to mammalian and fish counterparts, respectively. The phylogenetic tree showed that CiGal1-L2 was clustered with fish galectin-1s and closely related to *Cyprinus carpio*. Real-time quantitative PCR (RT-qPCR) analysis revealed that *CiGal1-L2* was widely expressed in all tested tissues. In addition, the expression of *CiGal1-L2* was differentially up-regulated challenged with grass carp reovirus (GCRV), lipopolysaccharide (LPS) and polyinosinic:polycytidylic acid (poly I:C). The fluorescence of CiGal1-L2-GFP was distributed in the cytoplasm and nucleus of HEK 293T cells and showed a trend of nuclear translocation after LPS and poly I:C treatment. Finally, the recombinant CiGal1-L2 (rCiGal1-L2) protein showed strong binding ability to LPS. In conclusion, the results provided further insight into the immune roles of galectin-1 in teleost.

1. Introduction

Grass carp (*Ctenopharyngodon idella*) has become an important economic freshwater species in China due to its excellent growth performance, wide adaptability and resistance to many infections [1,2]. However, grass carp is susceptible to infection with grass carp reovirus (GCRV), which causes severe hemorrhagic disease with approximately 85% mortality in fingerling and yearling grass carp in China [3–9]. The expression profile of Toll-like receptors of common carp (*Cyprinus carpio*) upon *Aeromonas hydrophila* challenge provided a fundament to disease-resistance selective breeding strategy development [10]. Therefore, a better understanding of innate immunity defense mechanisms could accelerate the breeding of disease-resistant strains of grass carp.

Galectins, as an evolutionary conserved group of lectin superfamily, are characterized by two properties: homologous carbohydrate-binding domain (CRD) and high affinity for β-galactoside. A number of animal galectins have been studied and 15 galectins have been identified in mammals. Based on their distinct molecular structures, galectins are classified into proto-, chimera-, and tandem-repeat-types [11]. Prototype subgroup (galectin-1, -2, -5, -7, -10, −11, −13, −14, and −15) contains only one CRD. In comparison, the tandem-repeat-type (galectin-4, -6, -8, -9, and -12) has two homologous CRDs joined by a short linker peptide. However, Chimera-type subgroup has a N-terminal domain rich in proline and glycine besides a *C*-terminal CRD, represented by a single member, galectin-3. Recently, galectins have a variety of biological functions in inflammation [12], cell adhesion and apoptosis [13], early embryogenesis [14], anti-cancer [15] and antiviral activity [16]. Especially, galectins are increasingly being proposed playing vital roles in adaptive and innate immunity [17,18]. Galectins are regarded

* Corresponding author. Institute of Hydrobiology, Chinese Academy of Sciences, Wuhan, 430072, PR China.
E-mail address: wangyp.ihb@gmail.com (Y. Wang).
[1] These authors contributed equally to this work as co-first authors.

https://doi.org/10.1016/j.fsi.2019.09.041
Received 16 May 2019; Received in revised form 10 September 2019; Accepted 16 September 2019
Available online 18 September 2019

as an important host pattern recognition receptors (PRRs). They can recognize and bind to pathogen-associated molecular patterns (PAMPs) of microbial pathogens including bacteria, fungi and virus by interacting with the β-galactoside [19]. They widely distribute in immune organs and immune cells [20].

Galectin-1, one of the prototype galectins, is the first protein discovered in the galectin family. Different from other galectins, the functions of galectin-1 have been well studied in mammals, especially its immune functions. With its specific immune functions, galectin-1 could regulate proliferation and apoptosis of T cell, and exhibit anti-inflammatory effect by blocking or attenuating signaling events [21,22]. Galectin-1 was shown to have anti-inflammatory activity by inhibiting leukocyte infiltration, migration and recruitment [22]. Moreover, galectin-1 was shown to bind to influenza virus and ameliorated pathogenesis [23]. At present, galectin-1 genes have been cloned and their functions involved immunity have been investigated in some bony fishes, such as orange-spotted grouper, flounder, bass, medaka, salmon, rainbow trout and pufferfish [24–30]. However, the study on the immune function of galectin-1 in grass carp is poorly understood.

Here, galectin 1-like 2 was isolated and characterized from *C. idella* (named as *CiGal1-L2*). The expression profiles of *CiGal1-L2* after various immune challenges and microbial ligand-binding activities of recombinant protein (rCiGal1-L2) were studied. The results provided further insight into the immune roles of galectin-1 in teleost.

2. Materials and methods

2.1. Ethics statement

All animal experiments were complied with the ARRIVE guidelines and were carried out in accordance with the National Institutes of Health guide for the care and use of Laboratory animals (NIH Publications No. 8023, revised 1978). All protocols were approved by the committee of the Institute of Hydrobiology, Chinese Academy of Sciences (CAS). The reference number obtained was Y11201-1-301 (Approval date: 30 May 2016). All surgeries were performed under eugenol anesthesia (final concentration: 100 mg/l) and all efforts were made to minimize suffering.

2.2. Experimental animals

Grass carp (3-month-old; weight, 10 ± 2 g; length, 7 ± 3 cm) were collected at the GuanQiao Experimental Station, Institute of Hydrobiology, Chinese Academic of Sciences, and acclimatized in aerated freshwater at 28 °C for one week. The fishes were fed with a commercial feed (Tong Wei, Chengdu, China) to adapt to the environment until 24 h before the experiments under the same conditions.

In the tissue distribution experiment, ten tissues, including liver, muscle, spleen, gill, intestine, skin, head kidney, middle kidney, heart and brain, were collected from 5 random untreated grass carp.

2.3. Immune challenge experiment

The PAMPs challenge experiments were performed as described previously [2]. Grass carp (n = 150) were randomly divided into three groups, including a control group, LPS and poly I:C challenge groups. 50 individuals of control group were intraperitoneally injected with 200 μlPBS (pH 7.4) while 50 individuals of each challenge groups were also intraperitoneally injected with an equal volume of LPS (L2880, Sigma, St. Louis, MO, USA, from *Escherichia coli* 055: B5, 0.5 mg/ml) or poly I:C (27 472 901, GE, 1 mg/ml) dissolved in PBS. These injected fish were kept under the same conditions as above mentioned. At 3, 6, 12, 24, and 48 h post injection (hpi), 5 individuals from each group were anaesthetized in eugenol anesthesia. The spleen and liver were harvested into TRIzol reagent (Invitrogen, Carlsbad, CA, USA) and stored at −80 °C until RNA extraction.

Table 1
Primers used in this study.

Primers	Sequences (5′—3′)	Purpose
Gal1-L2-F	ATGAGCGGTGTGATTGTGCAG	ORF cloning
Gal1-L2-R	TTACTTGATTTCAATTCCATAGATCTTG	
qGal1-L2-F	GCCCATGGTGACCACCACACT	RT-qPCR
qGal1-L2-R	TCAGCACCTTGACGGTTAGGGA	
qβ-actin-F	TCGGTATGGGACAGAAGGAC	
qβ-actin-R	GACCAGAGGCATACAGGGAC	
qS6-F	AGCGCAGCAGGCAATTACTATCT	GCRV RT-qPCR
qS6-R	ATCTGCTGGTAATGCGGAACG	

The GCRV challenge experiment was performed as described previously [5]. Briefly, 5 healthy grass carp were intraperitoneally injected with 200 μl PBS as control group while fish of challenge group were injected with an equal volume of GCRV (GD108 strain). The titer of virus detected by RT-qPCR (the special primers were listed in Table 1) was 3.12×10^3 copy/μl. These injected fish were kept under the same conditions as above mentioned. 5 individuals were collected at the indicated times post-infection, including 0, 1, 2, 3, 4, 5 and 6 days post-injection (dpi). The gill and liver were harvested into TRIzol reagent (Invitrogen) and stored at −80 °C until RNA extraction.

2.4. RNA isolation and cloning of CiGal1-L2

Total RNAs were extracted using TRIzol reagent according to previously study [31]. The *CiGal1-L2* gene was obtained by blasting the galectin-1 of zebrafish (Accession no. NM_212894.2) with the *C. idella* transcriptional database [32]. The coding sequence (CDS) was amplified using PCR primers (Table 1). The PCR products were purified, ligated into pMD18-T vectors (Takara, Japan), and transformed to *E. coli* DH5α (TransGen Biotech, Beijing, China) for sequencing by a commercial company (Tsing Ke, Wuhan, China).

2.5. Sequence analysis

The nucleotide and predicted amino acid sequences of CiGal1-L2 were analyzed using the Sequence Manipulation Suite (SMS) (http://www.bio-soft.net/sms/). Functional domains of the deduced amino acid sequence were predicted using on line SMART (http://smart.emblheidelberg.de/) [33]. Online SignaIP 4.0 Server (http://www.cbs.dtu.dk/services/SignalP/) was used to predict the signal peptide. The molecular weight (MW) and isoelectric point (pI) of the deduced amino acid sequence were calculated by ExPASy (http://web.expasy.org/compute_pi/). The conserved residues involved in carbohydrate binding activity were predicted by InterProScan (http://www.ebi.ac.uk/interpro/search/sequence-search). Analysis of amino acid sequence similarity of CiGal1-L2 with orthologous sequences using Geneious (version 8.1.3). The ClustalW2 (http://www.ebi.ac.uk/Tools/msa/clustalw2/) tool was engaged in performing the multiple sequences alignment. The phylogenetic position of CiGal1-L2 was assessed by reconstructing a phylogenetic tree using MEGA 5.0 program based on neighbor-joining (NJ) method with 1000 bootstraps [34].

2.6. Real-time quantitative PCR

The RNA extraction and cDNA synthesis were performed as a previous report [5]. All the samples of RNA were extracted from TRIzol reagent. 2 μg total RNA treated with RNase-free DNase I (Promega, Wisconsin, USA) was used for synthesizing first-strand cDNAs by ReverTra Ace kit (Toyobo, Osaka, Japan) and oligo (dT) primers in 20 μl reaction solution.

RT-qPCR was carried out using iQ™ SYBR Green Supermix (Bio-Rad, Hercules, CA, USA) on a CFX96™ Real Time Detection System (Bio-

Table 2
Primers used in this study.

Primers	Sequences (5′—3′)	Purpose
pEGFP-Gal1-L2-F	CTAGCGCTACCGGACTCAGATCTCGAG GTATGAGCGGTGTGATTGTGCAG	Subcellular localization
pEGFP-Gal1-L2-R	GCTCACCATGGTGGCGATGGATCCCTT GATTTCAATTCCATAGATCTTG	
pEASY-Gal1-L2-F	ATGTCTGCTGGAAACGCTAAGAT	Recombinant expression
pEASY-Gal1-L2-R	TTACTGCTTGGAGAAGAACTCCTT	

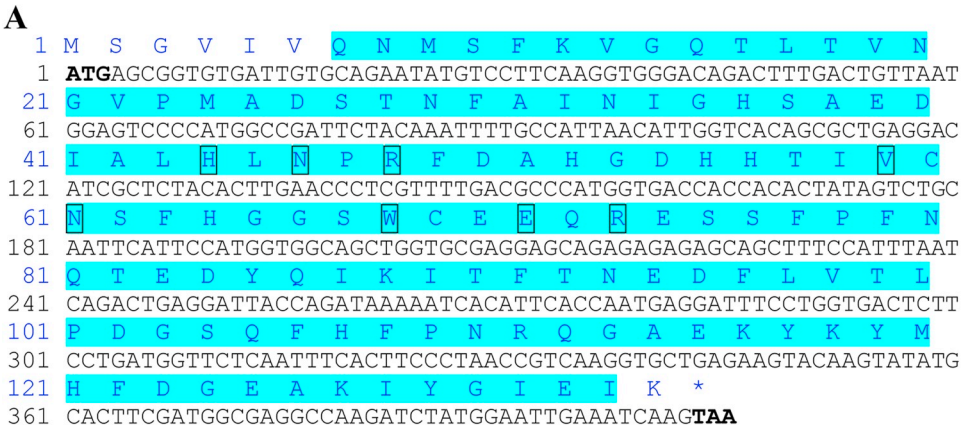

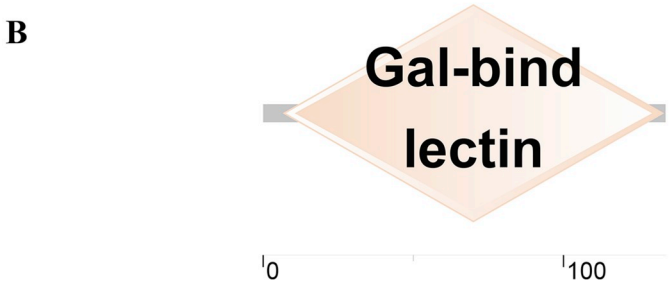

Fig. 1. (A) Nucleotide and deduced amino acid sequences of *CiGal1-L2*. The nucleotide sequence (lower) and the deduced amino acid sequence (upper) were numbered. The start codon (ATG) and stop codon (TAG) were represented in bold. The GLECT/Gal-bind_lectin domain was in dark green. The conserved residues involved in carbohydrate binding activity were boxed. (B) Schematic diagram of CiGal1-L2 functional domains. The GLECT/Gal-bind_lectin domain was predicted using online SMART. (For interpretation of the references to colour in this figure legend, the reader is referred to the Web version of this article.)

Rad). A pair of gene-specific primers (Table 1) were used to amplify the *CiGal1-L2* fragment. The β-actin of grass carp (Accession No. M25013.1) was selected as internal control and amplified with its specific primers (Table 1). The RT-qPCR cycling conditions as following: 95 °C for 2 min, 40 cycles of 95 °C for 10 s, annealing at 62 °C for 20 s, and 72 °C for 30 s, followed by a Melt Curve was constructed. Finally, the Ct values for respective reaction were subjected to comparative Ct method ($2^{-\Delta\Delta CT}$) [35] to calculate the relative expression of *CiGal1-L2*. Statistical analysis was conducted using one-way ANOVA by SPSS 16.0 and a probability level of $p \leq 0.05$ was considered as statistically significant.

2.7. Cell line and subcellular localization

Human embryonic kidney 293T (HEK 293T) cells were cultured in high glucose Dulbecco's modified Eagle's medium (DMEM; Hyclone, Logan, UT, USA), with 10% fetal bovine serum (FBS), 100 IU/ml penicillin (Sigma) and 100 mg/ml streptomycin (Sigma) under a humidified condition with 5% CO_2 at 37 °C. Transfection of plasmids in HEK 293T cells was performed using Lipo6000™ Transfection Reagent (Beyotime, Shanghai, China).

To study the distribution of *CiGal1-L2*, CiGal1-L2-pEGFP vector was constructed. Specific primers (Table 2) were designed to amplify the complete ORF sequence of *CiGal1-L2*. Then, the PCR product was cloned into pEGFP-N3 vectors (Clontech, Palo Alto, California, USA) using ClonExpress II One Step Cloning Kit (Vazyme Biotech Co., Ltd., Nanjing, China) and produced GFP-tagged expression plasmids. Sequence of the resulting plasmid was verified by DNA sequencing. HEK 293T cells were seeded into 6-well plates with 1×10^6 cells per well and cultured 24 h. After that, 5 μg of plasmid constructs of CiGal1-L2-pEGFP and pEGFP-N3 (vector control) were respectively transfected into the cells using Lipo6000™ Transfection Reagent. At 24 h post-transfection, the cells were fixed with 4% (v/v) paraformaldehyde, permeabilized with 0.2% Triton X-100, and stained with Hoechst 33342 (Beyotime) [31]. The cells were observed using the UltraVIEW VOX confocal system (PerkinElmer, Fremont, CA, USA) and a 63× oil immersion objective lens.

To evaluate the influence of PAMPs stimulation on subcellular localization of CiGal1-L2-GFP proteins, HEK293T cells were transfected with CiGal1-L2-GFP fusion plasmid or control plasmid (pEGFP-N3) and seeded into six-well plates. Approximately 24 h later, the cells were treated with 50 mg/ml poly I:C and 20 mg/ml LPS, respectively. After PAMPs stimulation, the HEK293T cells were observed using confocal system.

2.8. Overexpression and purification of rCiGal1-L2

To purify the recombinant CiGal1-L2, the complete ORF sequence of *CiGal1-L2* was amplified with specific primers (Table 2), then ligated into pEASY-Blunt cloning vector (TransGen Biotech). The recombinant plasmid was transformed into *E. coli* BL 21 (transsetta DE3) competent cells (TransGen Biotech), and confirmed by sequencing. *E. coli* BL21 transformed cells were cultured in 500 ml lysogeny broth (LB) with ampicillin (100 μg/ml) at 37 °C until ~0.6 OD600 reached. Cells were induced with isopropyl-β-thiogalactopyranoside (IPTG, at a final concentration of 1 mM) for 10 h at 20 °C. Subsequently, cells were kept on ice for 30 min and pelleted by centrifugating (4000 × g for 20 min at

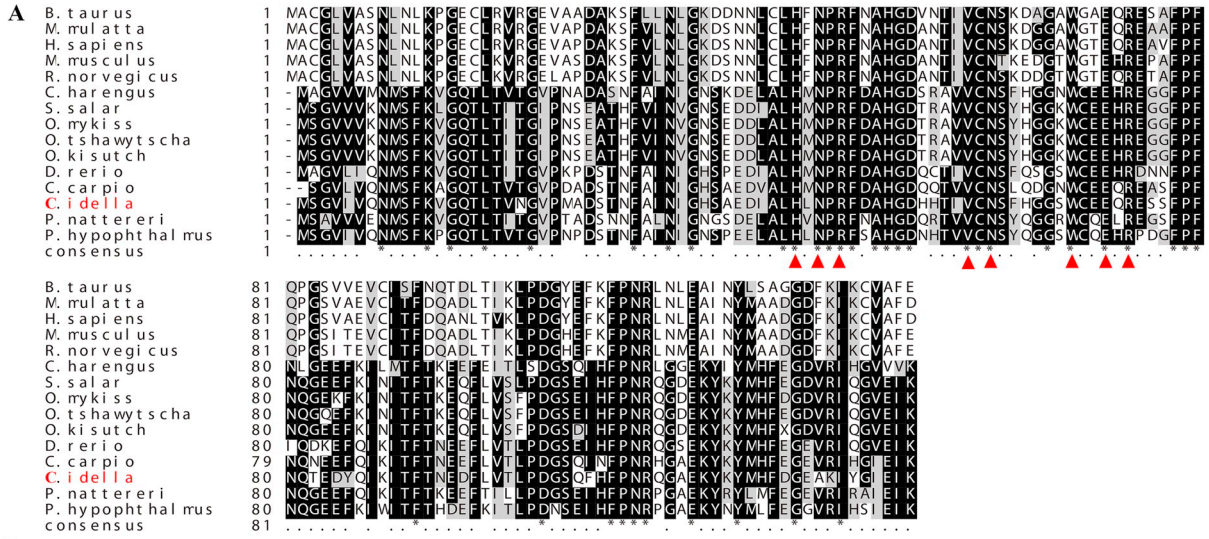

B

	The Species Name	Percents of Similarity														
		1	2	3	4	5	6	7	8	9	10	11	12	13	14	15
Percents of Similarity	1. O.mykiss		97.80	97.76	96.27	75.37	67.91	68.42	70.15	68.66	67.91	41.79	42.54	41.79	41.04	38.06
	2. O.kisutch	97.80		97.80	96.30	76.15	67.20	69.21	70.18	68.69	67.94	40.33	41.08	40.33	39.59	37.35
	3. O.tshawytscha	97.76	97.80		97.01	76.12	66.42	69.17	71.64	69.40	68.66	41.04	41.79	41.04	40.30	38.06
	4. S.salar	96.27	96.30	97.01		76.12	67.91	70.68	72.39	69.40	69.40	41.04	41.79	41.04	40.30	38.06
	5. C.harengus	75.37	76.15	76.12	76.12		66.42	71.43	68.66	70.90	71.64	41.79	41.04	41.04	41.04	40.30
	6. C.idella	67.91	67.20	66.42	67.91	66.42		81.20	76.87	67.16	70.15	42.54	42.54	40.30	41.79	41.04
	7. C.carpio	68.42	69.21	69.17	70.68	71.43	81.20		80.45	72.93	73.68	39.10	39.85	37.59	39.10	37.59
	8. D.rerio	70.15	70.18	71.64	72.39	68.66	76.87	80.45		68.66	71.64	38.81	39.55	38.06	38.81	36.57
	9. P.nattereri	68.66	68.69	69.40	69.40	70.90	67.16	72.93	68.66		74.63	42.54	41.79	41.04	41.79	41.79
	10.P.hypophthalmus	67.91	67.94	68.66	69.40	71.64	70.15	73.68	71.64	74.63		41.79	41.04	40.30	41.04	38.81
	11. M.mulatta	41.79	40.33	41.04	41.04	41.79	42.54	39.10	38.81	42.54	41.79		97.78	90.37	92.59	88.89
	12. H.sapiens	42.54	41.08	41.79	41.79	41.04	42.54	39.85	39.55	41.79	41.04	97.78		88.15	90.37	86.67
	13. M.musculus	41.79	40.33	41.04	41.04	41.04	40.30	37.59	38.06	41.04	40.30	90.37	88.15		95.56	83.70
	14. R.norvegicus	41.04	39.59	40.30	40.30	41.04	41.79	39.10	38.81	41.79	41.04	92.59	90.37	95.56		85.19
	15. B.taurus	38.06	37.35	38.06	38.06	40.30	41.04	37.59	36.57	41.79	38.81	88.89	86.67	83.70	85.19	

Fig. 2. (A) Multiple sequence alignment of CiGal1-L2. Numbers of amino acid are listed on the left side of alignments. The black shade represents 100% identity, dark gray represented 80% identity. The red triangle indicates the critical conserved residues for carbohydrate binding (as H–N-R, V–N and W–E-R). (B) Analysis of amino acid sequence similarity of CiGal1-L2 with orthologous sequences using Geneious (version 8.1.3). Species and gene accession numbers as following: *Cyprinus carpio* (XP_018930790.1); *Danio rerio* (NP_998059.2); *Salmo salar* (NP_001134631.1); *Oncorhynchus mykiss* (ACO07656.1); *Pygocentrus nattereri* (XP_017568757.1); *Oncorhynchus tshawytscha* (XP_024236660.1); *Oncorhynchus kisutch* (XP_020328504.1); *Pangasianodon hypophthalmus* (XP_026765594.1); *Clupea harengus* (XP_012673876.1); *Macaca mulatta* (NP_001162098.1); *Bos taurus* (NP_786976.1); *Mus musculus* (NP_032521.1); *Homo sapiens* (NP_002296.1); *Rattus norvegicus* (NP_063969.1). (For interpretation of the references to colour in this figure legend, the reader is referred to the Web version of this article.)

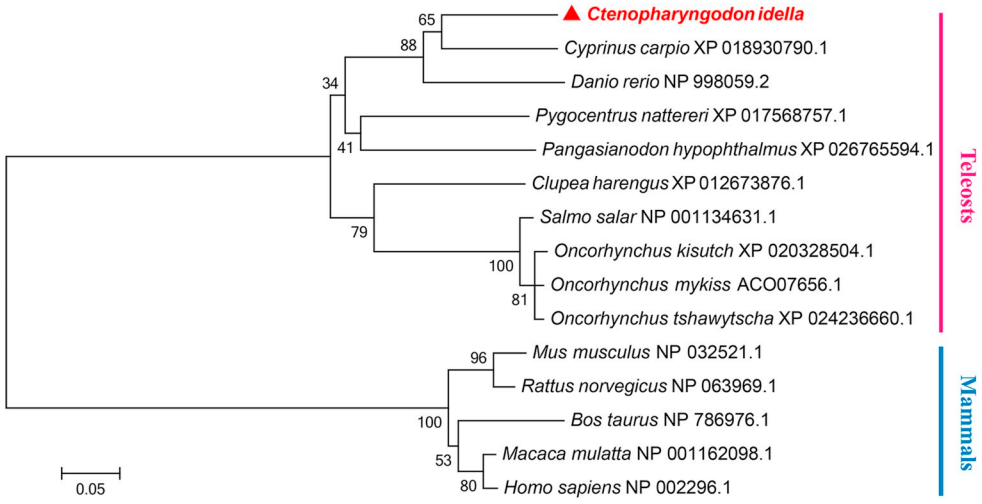

Fig. 3. The neighbor-joining phylogenetic tree of CiGal1-L2. The numbers are shown at each node state the bootstrap values (%). Species and gene accession numbers as follows: *Cyprinus carpio* (XP_018930790.1); *Danio rerio* (NP_998059.2); *Salmo salar* (NP_001134631.1); *Oncorhynchus mykiss* (ACO07656.1); *Pygocentrus nattereri* (XP_017568757.1); *Oncorhynchus tshawytscha* (XP_024236660.1); *Oncorhynchus kisutch* (XP_020328504.1); *Pangasianodon hypophthalmus* (XP_026765594.1); *Clupea harengus* (XP_012673876.1); *Macaca mulatta* (NP_001162098.1); *Bos taurus* (NP_786976.1); *Mus musculus* (NP_032521.1); *Homo sapiens* (NP_002296.1); *Rattus norvegicus* (NP_063969.1).

4 °C). Pelleted cells were resuspended in column buffer (20 mM Tris–HCl, pH 7.4, 200 mM NaCl) and stored overnight at −20 °C. Cell suspension was thawed and sonicated on ice in the presence of phenylmethane sulfonyl fluoride (PMSF, 1 mg/ml) protease inhibitor cocktail (Beyotime). Cells lysis was subjected to centrifugation (20 000 × g for 20 min at 4 °C) and the supernatant was purified with NI-NTA resign (TransGen Biotech). The recombinant proteins were analyzed by 12% SDS-PAGE and then transferred into a polyvinylidene difluoride

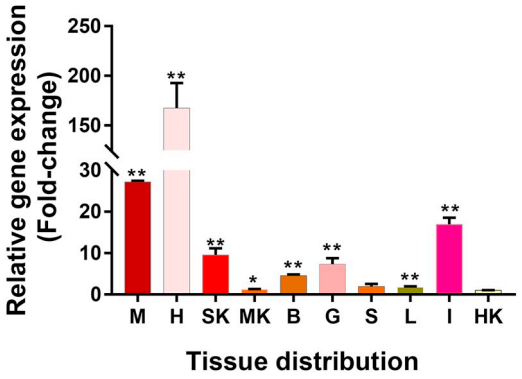

Fig. 4. Tissue distribution of *CiGal1-L2* transcript expression by RT-qPCR. The 10 examined tissues, including G, gill; SK, skin; B, brain; HK, head kidney; S, spleen; L, liver; M, muscle; MK, middle kidney; H, heart; I, intestine, were obtained from healthy grass carp ($n = 5$). The β-actin was used as an internal control. The expression level of *CiGal1-L2* in head kidney was set as 1, and mRNA expression levels in other tissues were expressed as fold changes relative to expression in the head kidney. All data were given in terms of relative mRNA expression as the mean ± SD. Asterisks (*) representative of significant difference (* = $p \leq 0.05$).

(PVDF) membrane (Millipore, Massachusetts, USA) using a Mini *Trans*-Blot electrophoretic transfer system (Bio-Rad, California, USA). Membranes were blocked with 5% non-fat milk (diluted with PBS containing 0.1% Tween-20) (PBST) for 2 h at room temperature, and then incubated with anti-His tag antibodies (diluted 1:5000 with 5% non-fat milk in PBST) for 8 h at 4 °C. After washing with PBST, the membranes were incubated with goat anti-rabbit IgG (Beyotime) (diluted 1:5000 with 5% non-fat milk in PBST) for 1 h at room temperature. The immunoblot signals were detected using an HRP-DAB Detection Kit (Tiangen, Beijing, China). Concentration of the purified protein was determined by using the BCA Protein Assay Kit (Novagen, Hilden, Germany). The gels were visualized by Coomassie blue R-250 staining.

2.9. Solid-phase enzyme-linked immunosorbent assay (ELISA)

The binding ability of recombinant CiGal1-L2 (rCiGal1-L2) with LPS was characterized by ELISA method as described previously [36]. Briefly, LPS (5 μg/ml) was coated to 96 microtiter plate at 4 °C overnight. The wells were washed with 300 μl PBST three times, and blocked with 100 μl 5% BSA at 4 °C for 1 h. Then, 100 μl of the increasing concentrations of purified rCiGal1-L2 (0.5, 1, 2, 4, 8 and 16 μg/mL) were added into each ligand-coated well, with four replicates for each concentration, and incubated at 37 °C for 1 h. Subsequently, the wells were incubated at 37 °C for 1 h with 100 μl HRP-labeled anti-His Monoclonal antibody (Proteintech Group, Inc., Chicago, IL, USA) (diluted 1:1000 in 5% BSA). Finally, the wells were incubated at 37 °C for 30 min with TMB Chromogen Solution (Beyotime), and then absorbances were read at 450 nm with an ELISA reader.

3. Results

3.1. Molecular characteristics and phylogenetic analysis of the full-length CiGal1-L2 gene

A 405 bp cDNA sequence was obtained by PCR from *C. idella* (Fig. 1A). The ORF of *CiGal1-L2* encoded a putative protein of 134 amino acids, with a predicted molecular mass of 15.143 kDa and an isoelectric point of 5.33. Structure prediction by SMART showed that the CiGal1-L2 protein had a Gal-bind lectin domain (also named CRD) and was absent from the signal peptide (Fig. 1B). The sugar binding motifs (H–N-R, V–N and W–E-R) involved in carbohydrate binding activity were detected in CRD (Fig. 1A; 2A). Multiple alignments revealed that the CRD has highly similarity among various species. The amino acid sequence similarity showed that CiGal1-L2 was 40.30–42.54% and 66.42–81.20% similarity to mammalian and fish counterparts, respectively (Fig. 2B), with the highly similarity to *C. carpio* (81.20%). The evolutionary tree showed that CiGal1-L2 was clustered with fish galectin1s and closely related to *C. carpio* (Fig. 3).

3.2. Tissue distribution analysis of CiGal1-L2

The tissue distribution of *CiGal1-L2* was examined in ten tissues by RT-qPCR using β-actin as the reference gene. The *CiGal1-L2* mRNA expressions in other tissues were expressed as fold changes relative to expression in the head kidney. The results indicated that *CiGal1-L2* was ubiquitously expressed in the tested tissues, however, its expression mainly distributed in heart (167.53-fold), muscle (27.23-fold), intestine (16.93-fold), skin (9.55-fold) and gill (7.33-fold) (Fig. 4).

3.3. Expression profile of CiGal1-L2 upon immune challenge

To detect the effect of GCRV infection, the relative copy number of the virus was examined in gill by RT-qPCR. The expression level of day 1 was set as the baseline (1.0). Special primers were designed based on the S6 segments of GCRV-II (special primers in Table 1). As shown in Fig. 5A, the relative copy number of GCRV was gradually raised from the time of infection, which implied that GCRV infection had occurred.

For the stimulation of GCRV, as shown in Fig. 5, the maximum transcriptions of *CiGal1-L2* were observed at 5 dpi in liver and gill (29.92-fold and 12.01-fold, respectively). After LPS injection, the mRNA levels of *CiGal1-L2* in LPS group were apparently up-regulated at 3, 6 and 48 hpi in spleen and at 3, 6 and 24 hpi in liver compared with the PBS group. After poly I:C injection, *CiGal1-L2* transcripts in spleen exhibited significant up-regulation from 3 to 48 hpi and peaked at 3

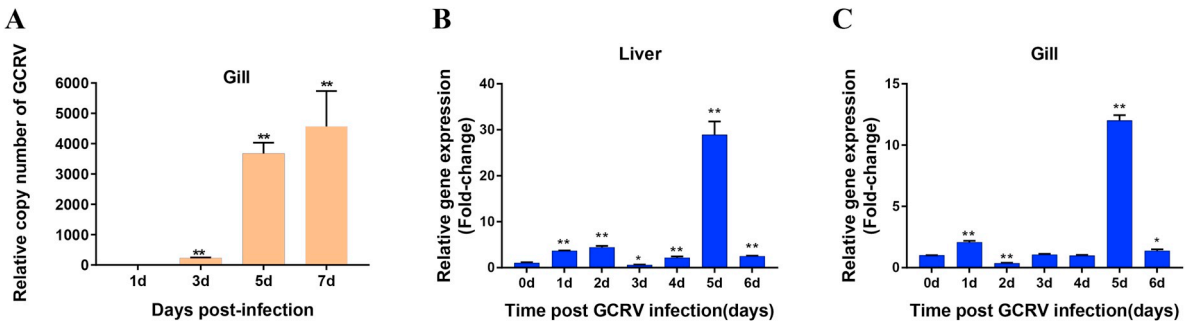

Fig. 5. (A) The relative number of GCRV copies was detected in gill. The relative number of GCRV copies on day 1 after infection was used as a reference for normalization. The β-actin was used as an internal control. (B–C) The mRNA expression patterns of *CiGal1-L2* in liver and gill after GCRV infection at 0–6 days. Expression levels on day 0 were used as control and set to 1.0. The β-actin was used as an internal control. All data were given in terms of relative mRNA expression as the mean ± SD (n = 5). Asterisks (*) representative of significant difference (* = $p \leq 0.05$, ** = $p \leq 0.01$).

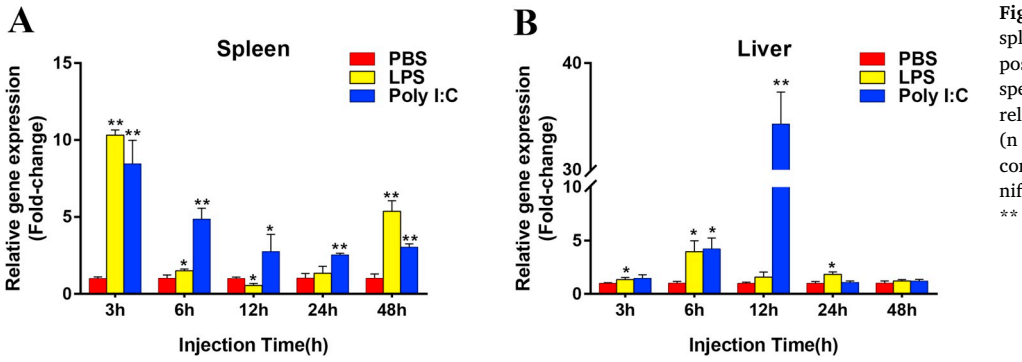

Fig. 6. Expression analysis of *CiGal1-L2* in the spleen (A), liver (B) at 3 h, 6 h, 12 h, 24 h, 48 h post-injection with PBS, LPS and poly I:C, respectively. All data were given in terms of relative mRNA expression as the mean ± SD (n = 5). The β-actin was used as an internal control. Asterisks (*) representative of significant difference (* = $p \leq 0.05$, ** = $p \leq 0.01$).

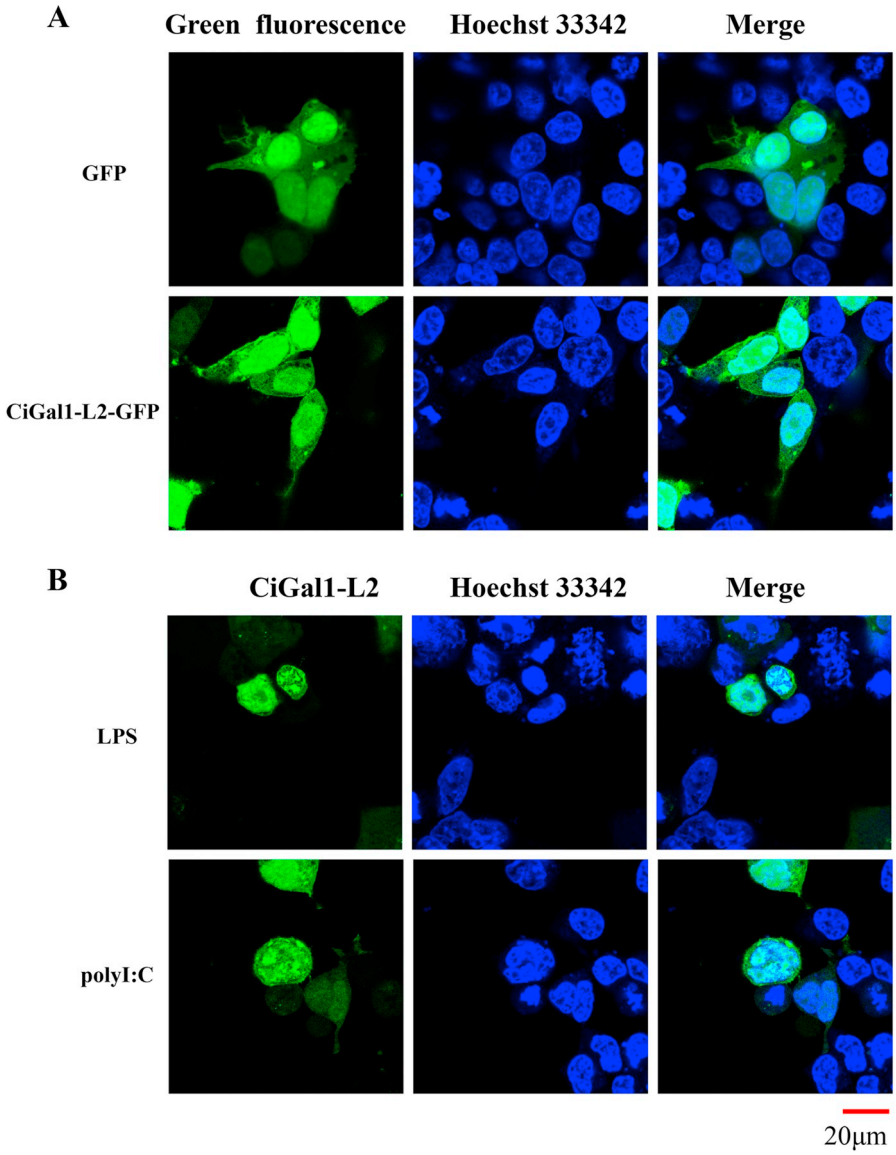

Fig. 7. (A) Subcellular localization of CiGal1-L2 proteins in HEK 293T cells (scale bar, 20 μm). (B) CiGal1-L2-GFP nuclear translocation induced by PAMPs stimulation (scale bar, 20 μm).

hpi. In liver, the transcription level kept a sustainable increase from 3 to 12 hpi, and reached a maximum induction of 34.30-fold at 12 hpi compared with the control group. Then, the transcription level was dropped to the initial levels from 24 to 48 hpi, and had no significantly difference with the control group (Fig. 6).

3.4. Subcellular localization of CiGal1-L2

To study the distribution of *CiGal1-L2*, CiGal1-L2-pEGFP eukaryotic expression vector was constructed and transfected into HEK 293T cells. Meanwhile, empty pEGFP-N3 plasmids were also transfected as the negative control. Same with the fluorescence pEGFP-N3 signal (Fig. 7A,

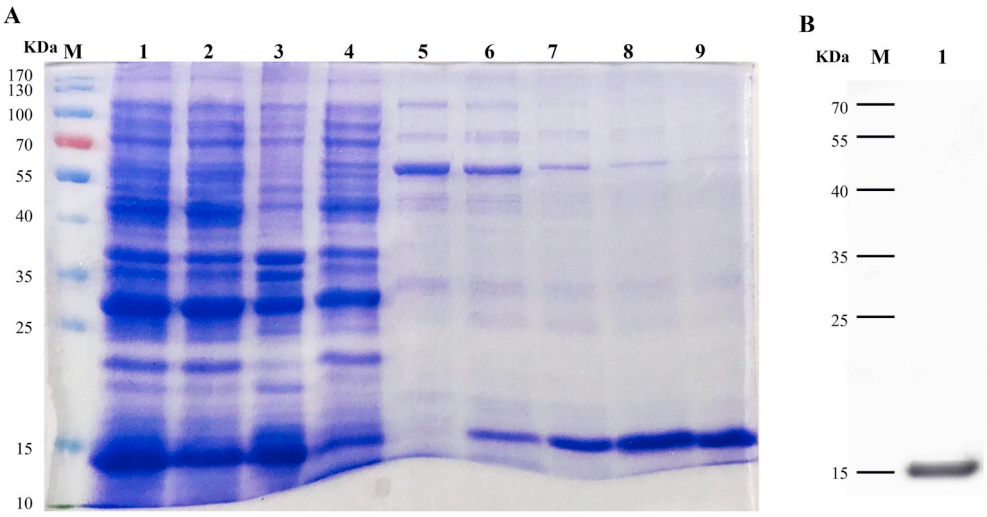

Fig. 8. (A) Sodium dodecyl sulfate-polyacrylamide gel electrophoresis (SDS-PAGE) analysis of CiGal1-L2 recombinant protein. Lane M: Protein molecular weight marker; lane 1: whole bacterial lysate after 6 h induction with 1.0 mM IPTG; lane 2: supernatant of lysate; lane 3, precipitation of lysate; lane 4, the passed lysate through Ni-NTA resin; lane 5–9, purified recombinant CiGal1-L2 protein washed from Ni-NTA resin with different concentrations of imidazole (40–200 mM). (B) Western blot analysis of recombinant CiGal1-L2 proteins in the *E. coli* BL21 (transsetta DE3) cells with anti-His-tag antibody. Lane M: Protein molecular weight marker; Lane 1: Purified recombinant CiGal1-L2 protein.

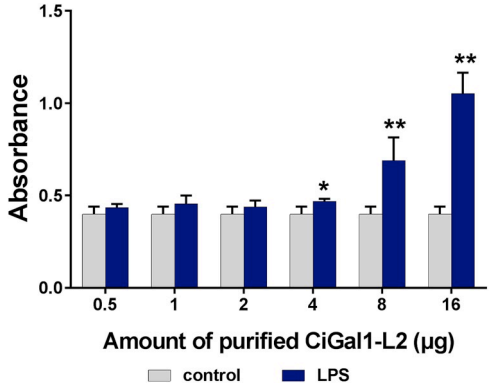

Fig. 9. Results of the binding assay of rCiGal1-L2 on LPS in vitro. * indicate a significant difference in the absorbance between LPS that exposed to rCiGal1-L2 and the control group (* = $p \leq 0.05$, ** = $p \leq 0.01$).

upper row), the fluorescence of CiGal1-L2-GFP was also distributed in the cytoplasm and nucleus of HEK 293T cells (Fig. 7A, lower row).

The effect of PAMPs stimulation on subcellular localization of CiGal1-L2-GFP proteins was shown in Fig. 7. After LPS and poly I:C stimulated the overexpressed CiGal1-L2-GFP cells, CiGal1-L2-GFP protein both showed a trend of nuclear translocation (Fig. 7B).

3.5. Expression of the rCiGal1-L2 protein

The rCiGal1-L2-6 × His tagged fusion protein was separated by SDS-PAGE, and an obvious band with a molecular weight of approximately 15 kDa was detected (Fig. 8A), which is consistent with the predicted molecular mass of rCiGal1-L2. When the rCiGal1-L2 was purified by Ni-NTA resin, Western blot analysis showed only one specific target protein with a molecular weight of 15 kDa (https://www.sciencedirect.com/science/article/pii/S1050464818301591, Fig. 8B). From the above results, rCiGal1-L2 expression and purification were successfully performed. The purified protein was used in the next experiment.

3.6. Microbial ligand-binding in vitro

The binding ability of CiGal1-L2 to microbial ligands was investigated to further characterize its immune function. In our results, the strong binding ability was observed to LPS with a dose-dependent manner compared with the control (Fig. 9), and the lowest dose of rCiGal1-L2 exhibiting significant binding ability was 4 μg/ml.

4. Discussion

Galectins are widely distributed in primary and secondary lymphoid organs and many types of immune cells, with vital roles in regulation of immune cell proliferation and apoptosis [20]. Galectin-1, one member of the galectin family, was up-regulated during inflammation and can act as modulators of innate defenses [37]. In the present study, the galectin-1 was cloned from *C. idella*. CiGal1-L2, an approximately 15.143 kDa protein, contains all the features characteristic of known galectin-1 proteins, including a β sandwich consisting of two anti-parallel β-sheets, and sugar binding motifs (H–N-R, V–N and W–E-R) highly conserved in CRD. It reveals that CiGal1-L2 is a proto-type galectin as other species galectin-1 [38]. From the multiple alignments among different species, CiGal1-L2 was similar to other galectin-1s, especially the CRD domain. Moreover, the phylogenetic tree showed that CiGal1-L2 was clustered with fish galectin-1s and closely related to *C. carpio*, which was in agreement with the traditional taxonomy. High conservation of structural elements and conserved phylogenetic relationship between CiGal1-L2 and other galectin-1s suggest its important biological functions in vertebrates.

Galectin-1 is abundant in the kidney, smooth muscle, thymus, skeletal muscle, sensory and motor neurons, myocardial and the placenta [39,40]. Some studies reported that galectins could mediate dendritic and macrophages cells adhere to other lectin activated lymphocyte, producing a following immune response mediated by IgG [41–43]. Galectin-1 plays double-acting role in cell adhesion regulation through combining with carbohydrate ligands of glycoprotein on the cell surface and extracellular matrix. In skeletal muscle, galectin-1 combines poly lactose amine chain of laminin, which influence fibronectin main receptor (integrin α, β1) identify laminin, and consequently inhibition of cell adhesion with the substrate contribute to the formation of muscle [44]. The galectin-1 of *Epinephelus coioides* (EcGal1) was mainly distributed in muscles and heart [24]. In this study, the *CiGal1-L2* mRNA was ubiquitously expressed in all tested tissues and highly distributed in heart and muscles, which was consistent with previous research. This indicates that *CiGal1-L2* may regulate grass carp cell adhesion. Moreover, higher expression patterns of *CiGal1-L2* in mucosal tissues (skin, gill and intestine), may relate to their vital roles for mucosal immune responses against pathogen infection.

In many species, galectin-1 has been shown to be involved in immune responses. For example, EcGal1 was expressed in the spleen, and challenge of the grouper with LPS, poly I:C and Singapore grouper iridovirus (SGIV) resulted in a differential up-regulation [24]. The expression of flounder galectin-1 was markedly increased from 24 h onwards, and the recombinant galectin-1 was able to neutralize the

lymphocystis disease virus (LCDV), inhibiting the formation of cytopathic effects [25]. Immunity challenges with *A. hydrophila* and Chinese giant salamander iridovirus (GSIV), the transcript level of *Andrias davidianus* galectin-1 (AdGal1) in kidney was significantly up-regulated [45]. Our results showed that *CiGal1-L2* was significantly induced by GCRV, LPS and poly I:C infection in the tested tissues of grass carp. The reason for the increasing transcription of *CiGal1-L2* after stimuli was possible that the existing *CiGal1-L2* in fish was recruited to translate into protein in response to stimulation. It suggests that *CiGal1-L2* is associated with the anti-viral and anti-bacteria response in grass carp. Moreover, CiGal1-L2-GFP protein showed a trend of nuclear translocation after LPS and poly I:C stimulated the overexpressed CiGal1-L2-GFP cells.

Finally, rCiGal1-L2 showed strong binding ability to LPS. As typical lectins, galectins possessed carbohydrate binding ability to microbial pathogens by recognizing exogenous ligands, especially carbohydrates on the surface of microbes via their CRDs, and subsequently triggered downstream immune signaling pathways to eliminate the pathogens [46,47]. In *A. davidianus*, rAdGal1 showed agglutination and binding activities to microbial bacteria, including Gram positive and Gram negative bacteria [45]. This indicates the crucial roles of rCiGal1-L2 as a PRR in the immune defense mechanism of grass carp.

In conclusion, the results of this study may provide valuable information for the study of the potential functional mechanism of galectin 1-like 2 in grass carp.

Acknowledgments

Funding: This work was supported by the National Natural Science Foundation of China (grant numbers 31572614 and 31721005).

References

[1] X.Y. Xu, Y.B. Shen, J.J. Fu, F. Liu, S.Z. Guo, J.L. Li, Characterization of MMP-9 gene from grass carp (Ctenopharyngodon idella): an Aeromonas hydrophila-inducible factor in grass carp immune system, Fish Shellfish Immunol. 35 (3) (2013) 801–807.
[2] D. Zhu, Y. Li, R. Huang, L. Luo, L. Chen, P. Fu, L. He, Y. Li, L. Liao, Z. Zhu, Y. Wang, Molecular characterization and functional activity of Prx1 in grass carp (Ctenopharyngodon Idella), Fish Shellfish Immunol. (2019).
[3] Q. Fang, H. Attoui, J.F.P. Biagini, Z.Y. Zhu, P. de Micco, X. de Lamballerie, Sequence of genome segments 1, 2, and 3 of the grass carp reovirus (genus Aquareovirus, family Reoviridae) (vol 274, pg 762, 2000), Biochem. Biophys. Res. Commun. 276 (1) (2000) 391.
[4] Y. Rao, J. Su, Insights into the antiviral immunity against grass carp (Ctenopharyngodon idella) reovirus (GCRV) in grass carp, J. Immunol. Res. 2015 (2015) 670437.
[5] D. Zhu, R. Huang, L. Chen, P. Fu, L. Luo, L. He, Y. Li, L. Liao, Z. Zhu, Y. Wang, Cloning and characterization of the LEF/TCF gene family in grass carp (Ctenopharyngodon idella) and their expression profiles in response to grass carp reovirus infection, Fish Shellfish Immunol. 86 (2019) 335–346.
[6] L. Chen, R. Huang, D. Zhu, Y. Wang, R. Mehjabin, Y. Li, L. Liao, L. He, Z. Zhu, Y. Wang, Cloning of six serpin genes and their responses to GCRV infection in grass carp (Ctenopharyngodon idella), Fish Shellfish Immunol. 86 (2019) 93–100.
[7] L. Luo, D. Zhu, R. Huang, L. Xiong, R. Mehjabin, L. He, L. Liao, Y. Li, Z. Zhu, Y. Wang, Molecular cloning and preliminary functional analysis of six RING-between-ring (RBR) genes in grass carp (Ctenopharyngodon idellus), Fish Shellfish Immunol. 87 (2019) 62–72.
[8] R. Mehjabin, L. Chen, R. Huang, D. Zhu, C. Yang, Y. Li, L. Liao, L. He, Z. Zhu, Y. Wang, Expression and localization of grass carp pkc-theta (protein kinase C theta) gene after its activation, Fish Shellfish Immunol. 87 (2019) 788–795.
[9] Y. Tian, X. Ye, L. Zhang, G. Deng, Y. Bai, Development of a novel candidate subunit vaccine against Grass carp reovirus Guangdong strain (GCRV-GD108), Fish Shellfish Immunol. 35 (2) (2013) 351–356.
[10] Y. Gong, S. Feng, S. Li, Y. Zhang, Z. Zhao, M. Hu, P. Xu, Y. Jiang, Genome-wide characterization of Toll-like receptor gene family in common carp (Cyprinus carpio) and their involvement in host immune response to Aeromonas hydrophila infection, Comp. Biochem. Physiol. Part D: Genom. Proteom. 24 (2017) 89–98.
[11] J. Hirabayashi, K. Kasai, The family of metazoan metal-independent beta-galactoside-binding lectins: structure, function and molecular evolution, Glycobiology 3 (4) (1993) 297–304.
[12] N. Rubinstein, J.M. Ilarregui, M.A. Toscano, G.A. Rabinovich, The role of galectins in the initiation, amplification and resolution of the inflammatory response, Tissue Antigens 64 (1) (2004) 1–12.
[13] J. Dumic, S. Dabelic, M. Flogel, Galectin-3: an open-ended story, Biochim. Biophys. Acta 1760 (4) (2006) 616–635.
[14] H. Ahmed, S.J. Du, N. O'Leary, G.R. Vasta, Biochemical and molecular characterization of galectins from zebrafish (Danio rerio): notochord-specific expression of a prototype galectin during early embryogenesis, Glycobiology 14 (3) (2004) 219–232.
[15] F. Cedeno-Laurent, C.J. Dimitroff, Galectins and their ligands: negative regulators of anti-tumor immunity, Glycoconj. J. 29 (8–9) (2012) 619–625.
[16] M. Nita-Lazar, J. Mancini, C. Feng, N. Gonzalez-Montalban, C. Ravindran, S. Jackson, A. de Las Heras-Sanchez, B. Giomarelli, H. Ahmed, S.M. Haslam, G. Wu, A. Dell, A. Ammayappan, V.N. Vakharia, G.R. Vasta, The zebrafish galectins Drgal1-L2 and Drgal3-L1 bind in vitro to the infectious hematopoietic necrosis virus (IHNV) glycoprotein and reduce viral adhesion to fish epithelial cells, Dev. Comp. Immunol. 55 (2016) 241–252.
[17] H.J. Gabius, Animal lectins, Eur. J. Biochem. 243 (3) (1997) 543–576.
[18] G.R. Vasta, Galectins as pattern recognition receptors: structure, function, and evolution, Adv. Exp. Med. Biol. 946 (2012) 21–36.
[19] G.R. Vasta, H. Ahmed, M. Nita-Lazar, A. Banerjee, M. Pasek, S. Shridhar, P. Guha, J.A. Fernandez-Robledo, Galectins as self/non-self recognition receptors in innate and adaptive immunity: an unresolved paradox, Front. Immunol. 3 (2012) 199.
[20] G.A. Rabinovich, L.G. Baum, N. Tinari, R. Paganelli, C. Natoli, F.T. Liu, S. Iacobelli, Galectins and their ligands: amplifiers, silencers or tuners of the inflammatory response? Trends Immunol. 23 (6) (2002) 313–320.
[21] G.A. Rabinovich, M.A. Toscano, Turning 'sweet' on immunity: galectin-glycan interactions in immune tolerance and inflammation, Nat. Rev. Immunol. 9 (5) (2009) 338–352.
[22] S.R. Stowell, Y.N. Qian, S. Karmakar, N.S. Koyama, M. Dias-Baruffi, H. Leffler, R.P. McEver, R.D. Cummings, Differential roles of galectin-1 and galectin-3 in regulating leukocyte viability and cytokine secretion, J. Immunol. 180 (5) (2008) 3091–3102.
[23] M.L. Yang, Y.H. Chen, S.W. Wang, Y.J. Huang, C.H. Leu, N.C. Yeh, C.Y. Chu, C.C. Lin, G.S. Shieh, Y.L. Chen, J.R. Wang, C.H. Wang, C.L. Wu, A.L. Shiau, Galectin-1 binds to influenza virus and ameliorates influenza virus pathogenesis, J. Virol. 85 (19) (2011) 10010–10020.
[24] X.L. Chen, J.G. Wei, M. Xu, M. Yang, P.F. Li, S.N. Wei, Y.H. Huang, Q.W. Qin, Molecular cloning and characterization of a galectin-1 homolog in orange-spotted grouper, Epinephelus coioides, Fish Shellfish Immunol. 54 (2016) 333–341.
[25] S.S. Liu, G.B. Hu, C. Sun, S.C. Zhang, Anti-viral activity of galectin-1 from flounder Paralichthys olivaceus, Fish Shellfish Immunol. 34 (6) (2013) 1463–1469.
[26] L. Poisa-Beiro, S. Dios, H. Ahmed, G.R. Vasta, A. Martinez-Lopez, A. Estepa, J. Alonso-Gutierrez, A. Figueras, B. Novoa, Nodavirus infection of Sea bass (Dicentrarchus labrax) induces up-regulation of galectin-1 expression with potential anti-inflammatory activity, J. Immunol. 183 (10) (2009) 6600–6611.
[27] G.R. Vasta, M. Nita-Lazar, B. Giomarelli, H. Ahmed, S.J. Du, M. Cammarata, N. Parrinello, M.A. Bianchet, L.M. Amzel, Structural and functional diversity of the lectin repertoire in teleost fish: relevance to innate and adaptive immunity, Dev. Comp. Immunol. 35 (12) (2011) 1388–1399.
[28] G.R. Vasta, H. Ahmed, E.W. Odom, Structural and functional diversity of lectin repertoires in invertebrates, protochordates and ectothermic vertebrates, Curr. Opin. Struct. Biol. 14 (5) (2004) 617–630.
[29] G.R. Vasta, H. Ahmed, S.J. Du, D. Henrikson, Galectins in teleost fish: zebrafish (Danio rerio) as a model species to address their biological roles in development and innate immunity, Glycoconj. J. 21 (8–9) (2004) 503–521.
[30] M.K. Chen, X. Liu, J. Zhou, X. Wang, R.T. Liu, H.Y. Peng, B.Y. Li, Z.L. Cai, C. Jiang, Molecular characterization and expression analysis of galectins in Japanese pufferfish (Takifugu rubripes) in response to Vibrio harveyi infection, Fish Shellfish Immunol. 86 (2019) 347–354.
[31] D. Zhu, R. Huang, P. Fu, L. Chen, L. Luo, P. Chu, L. He, Y. Li, L. Liao, Z. Zhu, Y. Wang, Investigating the role of BATF3 in grass carp (Ctenopharyngodon idella) immune modulation: a fundamental functional analysis, Int. J. Mol. Sci. 20 (7) (2019) 1687.
[32] Y. Wang, Y. Lu, Y. Zhang, Z. Ning, Y. Li, Q. Zhao, H. Lu, R. Huang, X. Xia, Q. Feng, X. Liang, K. Liu, L. Zhang, T. Lu, T. Huang, D. Fan, Q. Weng, C. Zhu, Y. Lu, W. Li, Z. Wen, C. Zhou, Q. Tian, X. Kang, M. Shi, W. Zhang, S. Jang, F. Du, S. He, L. Liao, Y. Li, B. Gui, H. He, Z. Ning, C. Yang, L. He, L. Luo, R. Yang, Q. Luo, X. Liu, S. Li, W. Huang, L. Xiao, H. Lin, B. Han, Z. Zhu, The draft genome of the grass carp (Ctenopharyngodon idellus) provides insights into its evolution and vegetarian adaptation, Nat. Genet. 47 (6) (2015) 625–631.
[33] I. Letunic, T. Doerks, P. Bork, SMART: recent updates, new developments and status in 2015, Nucleic Acids Res. 43 (2015) D257–D260 (Database issue).
[34] K. Tamura, D. Peterson, N. Peterson, G. Stecher, M. Nei, S. Kumar, MEGA5: molecular evolutionary genetics analysis using maximum likelihood, evolutionary distance, and maximum parsimony methods, Mol. Biol. Evol. 28 (10) (2011) 2731–2739.
[35] K.J. Livak, T.D. Schmittgen, Analysis of relative gene expression data using real-time quantitative PCR and the 2(T)(-Delta Delta C) method, Methods 25 (4) (2001) 402–408.
[36] J. Chen, L. Zhang, N. Yang, M. Tian, Q. Fu, F. Tan, C. Li, Expression profiling and microbial ligand binding analysis of galectin-4 in turbot (Scophthalmus maximus L.), Fish Shellfish Immunol. 84 (2019) 673–679.
[37] S. Gauthier, I. Pelletier, M. Ouellet, A. Vargas, M.J. Tremblay, S. Sato, B. Barbeau, Induction of galectin-1 expression by HTLV-I Tax and its impact on HTLV-I infectivity, Retrovirology 5 (2008).
[38] M.T. Elola, M.E. Chiesa, A.F. Alberti, J. Mordoh, N.E. Fink, Galectin-1 receptors in different cell types, J. Biomed. Sci. 12 (1) (2005) 13–29.
[39] D.C. Kilpatrick, Animal lectins: a historical introduction and overview, Biochim. Biophys. Acta 1572 (2–3) (2002) 187–197.

[40] E.L. Levroney, H.C. Aguilar, J.A. Fulcher, L. Kohatsu, K.E. Pace, M. Pang, K.B. Gurney, L.G. Baum, B. Lee, Novel innate immune functions for galectin-1: galectin-1 inhibits cell fusion by Nipah virus envelope glycoproteins and augments dendritic cell secretion of proinflammatory cytokines, J. Immunol. 175 (1) (2005) 413–420.
[41] K. Goldring, G.E. Jones, R. Thiagarajah, D.J. Watt, The effect of galectin-1 on the differentiation of fibroblasts and myoblasts in vitro, J. Cell Sci. 115 (Pt 2) (2002) 355–366.
[42] A. Paz, R. Haklai, G. Elad-Sfadia, E. Ballan, Y. Kloog, Galectin-1 binds oncogenic H-Ras to mediate Ras membrane anchorage and cell transformation, Oncogene 20 (51) (2001) 7486–7493.
[43] F. van den Brule, S. Califice, V. Castronovo, Expression of galectins in cancer: a critical review, Glycoconj. J. 19 (7–9) (2002) 537–542.
[44] D.N.W. Cooper, Galectin-1: secretion and modulation of cell interactions with laminin, Trends Glycosci. Glycotechnol. 9 (45) (1997) 57–67.
[45] H. Yang, Q. Lan, R. Liu, D. Cui, H. Liu, D. Xiong, F. Li, X. Liu, L. Wang, Characterization of galectin-1 from Chinese giant salamanders Andrias davidianus and its involvements during immune response, Dev. Comp. Immunol. 70 (2017) 59–68.
[46] S. Kamhawi, M. Ramalho-Ortigao, V.M. Pham, S. Kumar, P.G. Lawyer, S.J. Turco, C. Barillas-Mury, D.L. Sacks, J.G. Valenzuela, A role for insect galectins in parasite survival, Cell 119 (3) (2004) 329–341.
[47] X.Y. Song, H. Zhang, L.L. Wang, J.M. Zhao, C.K. Mu, L.S. Song, L.M. Qiu, X.L. Liu, A galectin with quadruple-domain from bay scallop Argopecten irradians is involved in innate immune response, Dev. Comp. Immunol. 35 (5) (2011) 592–602.